Gas-phase Observations of Accretion Products from Stabilized Criegee Intermediates in Terpene Ozonolysis with Two Dicarboxylic Acids

Yuanyuan Luo[1, *], Lauri Franzon[2], Jiangyi Zhang[1], Nina Sarnela[1], Neil M. Donahue[3], Theo Kurtén[2], and Mikael Ehn[1, *]

[1] Institute for Atmospheric and Earth System Research (INAR), University of Helsinki, Helsinki, 00014, Finland
[2] Department of Chemistry, University of Helsinki, Helsinki, 00014, Finland
[3] Center for Atmospheric Particle Studies, Carnegie Mellon University, Pennsylvania, 15213, United States

Correspondence to: Yuanyuan Luo (yuanyuan.luo@helsinki.fi) and Mikael Ehn (mikael.ehn@helsinki.fi)

Keywords: Criegee intermediates, terpenes, accretion products, carboxylic acids

Abstract.

Criegee intermediates (CIs), forming from the ozonolysis of alkenes, are highly reactive species with diverse reaction pathways, with important roles in atmospheric chemistry. This study focuses on the formation of accretion products through reactions of thermally stabilized CIs (sCIs) from the ozonolysis of three different terpenes (α-pinene, β-pinene, and β-caryophyllene) with malonic and oxalic acids. Our experimental results demonstrate that these reactions efficiently produce the expected accretion products, though with apparent variations in yields depending on the specific terpene and acid involved. To our knowledge, this is the first study to report direct gas-phase observations of expected adducts from several different terpene-derived sCIs and carboxylic acids, paving the way for a better understanding of the importance and atmospheric implications of these reactions, especially in terms of aerosol-forming capabilities of these large product molecules.

1. Introduction

Stabilized Criegee intermediates (sCIs), which are formed from the stabilization of excited Criegee intermediates (eCIs) during the ozonolysis of alkenes, play diverse roles in tropospheric chemistry. Depending on their structure, sCIs can have fast unimolecular reaction rates (Long et al., 2016; Chhantyal-Pun et al., 2015; Lester and Klippenstein, 2018; Drozd and Donahue, 2011), but also react with various trace atmospheric species, including water vapor, sulfur dioxide (SO_2), nitrogen oxides (NO_x), carboxylic acids, and carbonyl compounds (Cox et al., 2020; Osborn and Taatjes, 2015; Khan et al., 2018; Lin and Chao, 2017; Chhantyal-Pun et al., 2020; Gong and Chen, 2021; Taatjes et al., 2013). These reactions can produce low-volatility species that significantly contribute to the formation of both inorganic and organic aerosol components, consequently impacting air quality, climate, and human health.

Carboxylic acids are emitted directly into the atmosphere from both biogenic and anthropogenic sources and can also be produced in situ through various photochemical reactions. Observations have shown that carboxylic acids can maintain steady-state mixing ratios of up to a few parts per billion by volume (ppbv) at different locations globally (Kawamura et al., 1985; Chebbi and Carlier, 1996; Khan et al., 2015). Organic acids can react with stabilized sCIs to form adducts (Welz et al., 2014), facilitating a pathway through which alkenes are transformed into low-volatility compounds, thus contributing to the formation of secondary organic aerosol (SOA) (Chhantyal-Pun et al., 2018; Khan et al., 2018). Calculations on the reaction of formic acid with sCIs indicate that sCIs can target both the hydroxyl group and the carbonyl bond, forming stable adducts like peroxyesters, with the hydroxyl group attack being more favorable due to its higher exothermicity (Vereecken, 2017; Vereecken and Francisco, 2012). Recent direct kinetic investigations have measured reaction rate coefficients between sCIs and organic acids, finding values that greatly exceed those predicted by earlier theoretical computations or analyses of reaction end products (Chhantyal-Pun et al., 2017; Elsamra et al., 2016; Chhantyal-Pun et al., 2018). These studies have demonstrated that reactions of sCIs with carboxylic acids are typically at the gas-kinetic collision limit (Vereecken et al., 2014; Chhantyal-Pun et al., 2018).

While the significance of reactions between sCIs and organic acids has long been recognized, only recently has it become possible to measure some fundamental sCIs, enabling further experimental investigations into their properties and roles in the atmosphere (Sheps et al., 2014; Taatjes et al., 2013; Welz et al., 2014; Welz et al., 2012). Despite these advancements, the wide variety of carboxylic acids in the atmosphere, coupled with the diverse sCIs generated through the ozonolysis of alkenes, results in numerous potential reaction products. Identifying specific reaction pathways and products is especially challenging for sCIs from complex molecules like terpenes, which are a major source of atmospheric SOA (Lee et al., 2006; Yang et al., 2021; Faiola et al., 2018). Although many studies have posited that sCIs from such complex molecules reacting with organic acids could significantly contribute to the formation of SOA (Gong and Chen, 2021; Gong et al., 2024; Vansco et al., 2020; Yao et al., 2014; Wang et al., 2016), direct gas-phase observations of products from reactions involving larger sCIs—particularly those derived from monoterpenes and sesquiterpenes —are still extremely limited. Several papers have reported on the use of acids to scavenge sCIs (Berndt et al., 2017; Yao et al., 2014; Gong and Chen, 2021). However, these studies have

primarily focused on the kinetics of sCIs and/or their role in aerosol formation, and therefore not tried to look into the formed products. Berndt et al. (2018) reported the formation of an abundant product from monoterpene sCI + acetic acid, but the data was not explicitly shown in that study. Even for smaller sCIs, very few direct observations of the expected products have been presented. Vansco et al. (2020) demonstrated the formation of functionalized hydroperoxide adducts from reactions between isoprene-derived sCIs and formic acid using multiplexed photoionization mass spectrometry.

In our previous work on the ozonolysis of the diterpene kaurene (Luo et al., 2022), we identified a series of oxidation products containing 21-29 carbon atoms, as depicted in Figure 1(a). Initially, we hypothesized that these products might have formed from cross-reactions of peroxy radicals (RO_2) from kaurene with smaller RO_2 formed from OH oxidation of various C_{2-9} organic contaminants within the chamber (Figure 1 (c)). However, we have later come to hypothesize that these might in fact have been products of sCIs with organic acid contaminants. Given that prior studies suggest a higher fraction of sCIs in larger molecules (Hakala and Donahue, 2023; Vereecken, 2017), we decided that this data is worth re-analyzing. To investigate sCI accretion products further, we conducted experiments in a flow tube reactor focusing on terpene-derived sCIs reacting with carboxylic acids. We used three different terpenes—α-pinene, β-pinene, and β-caryophyllene—and two commonly measured ambient dicarboxylic acids, malonic and oxalic acids, to explore sCIs' accretion pathways with acids across these chemical systems.

2. Materials and Methods

2.1. Laboratory Experiments

We conducted experiments in a flow reactor at room temperature under dry conditions. The total flow was set at 16 L min^{-1}, generated using a zero-air generator (AADCO, Series 737-14, Ohio, USA), resulting in a residence time of approximately 3 s. We utilized three different terpenes in each experiment: two monoterpenes, α-pinene and β-pinene (both $C_{10}H_{16}$), and one sesquiterpene, β-caryophyllene ($C_{15}H_{24}$), of which the structures are shown in Figure S1. These were introduced into the flow reactor using a syringe pump setup, while ozone was added to the reactor from a Dasibi 1008-PC ozone generator. Once the terpene oxidation product signals had stabilized, we added either malonic acid ($C_3H_4O_4$) or oxalic acid ($C_2H_2O_4$) to titrate the sCIs. These dicarboxylic acids were chosen to enhance the detection of accretion products using our nitrate ion-based chemical ionization mass spectrometer (hereafter NO_3-CIMS). Dicarboxylic acids were chosen because they were expected to produce accretion products with functionalities that were detectable by the NO_3-CIMS. The acids were vaporized into the reactor by flushing N_2 through a vial containing the solid acid, which was heated (~60 °C) using a water bath to promote evaporation.

Ozone concentrations were monitored using a UV photometric analyzer (model 49P, Thermo Environmental). Terpene concentrations were measured by a Vocus proton-transfer-reaction time-of-flight mass spectrometer (Vocus PTR, Tofwerk AG) (Krechmer et al., 2018), which was calibrated daily with a gas-phase standard (Apel-Riemer Environmental, Inc) containing 19 components, including α-pinene. The sensitivity for α-pinene was determined as 1370 ± 280 cps ppb^{-1}. Since β-pinene and β-caryophyllene were not included in the standard, their sensitivities were estimated based on their proton affinity,

85 fragmentation patterns, and transmission efficiencies, yielding sensitivities of 1400 ± 289 cps ppb^{-1} for β-pinene and 1780 ± 368 cps ppb^{-1} for β-caryophyllene, respectively. Highly oxygenated organic molecules (HOMs), accretion products, and carboxylic acids were detected using NO$_3$-CIMS (Tofwerk AG/Aerodyne Research Inc.), which has been shown to be very sensitive towards highly oxygenated species, typically with two or more H-bond donors (Junninen et al., 2010; Hyttinen et al., 2015). For such species, the charging is typically assumed to be collision limited. The NO$_3$-CIMS was not directly calibrated

90 in this study, owing to various challenges related to HOM quantification (Riva et al., 2019), but a calibration factor of 1×10^{10} cm^{-3} was used to provide a rough estimate of product concentrations. This naturally introduces a large uncertainty, estimated as at least a factor of 3, but our focus will be on species identification and on comparing relative concentration changes, meaning that the lack of detailed quantification will not hamper our conclusions. Data from all instruments were collected at a frequency of 1 Hz. Data from both the Vocus PTR-TOF and NO$_3$-CIMS were analyzed using the MATLAB tofTools package

95 (version 612) (Junninen, 2014).

2.2. Quantum Calculation

The simplified mechanism of the formation of accretion product from CIs + carboxylic acid reaction is shown in Scheme 1. Quantum chemical calculations were performed to help explain the experimental observations. Reaction rate coefficients with both dicarboxylic acids were estimated for all the α-pinene and β-pinene derived sCIs, and Gibbs free energies of clustering

100 with the nitrate ion were calculated for the accretion products derived from these. β-caryophyllene-derived sCIs were not considered due to the power law dependence of computational cost on molecular size.

In a previous computational study, Vereecken found that gas-phase reactions between sCI and simple carboxylic acids are collision-limited using microvariational transition state theory (Vereecken, 2017). We considered such calculations to be beyond the scope of this work due to having a high computational cost for the C$_9$ and C$_{10}$ sCIs, and simply performed a few

105 test calculations to confirm that the sCI + dicarboxylic acid mechanism proceeds similarly to Vereecken's sCI + HCOOH mechanism, and used the dipole moment-based Structure-Activity Relationship (SAR) by Chhantyal-Pun et al. (2018) to estimate reaction rate coefficients. Detailed results and method descriptions on these calculations are found in the Supplementary Information.

The Gibbs free energies of clustering with the NO$_3^-$ ion for the α-pinene and β-pinene derived accretion products were

110 calculated similarly as in Hyttinen et al. (2015). The final Gibbs free energies of clustering were compared to the corresponding value for HNO$_3$ to determine the detectability of each accretion product in our experimental conditions. The results are presented in Table S3.

In the computations, conformer sampling of all species was performed using the XTB-GFN2 level of theory with the CREST software (Pracht et al., 2024). For the quantum chemical calculations, geometry optimizations were performed using various

115 density functionals (See Supplementary Information for more details), and final single-point electronic energy corrections with DLPNO/CCSD(T). These quantum chemical calculations were performed using the ORCA program, versions 5.0.4 and 6.0 (Neese, 2022, 2023). Full details of all performed computations can be found in the Supplementary Information.

Scheme 1. The Criegee Intermediate + Carboxylic Acid reaction forms an α-acyloxy hydroperoxide accretion product.

3. Results and Discussion

The different sCIs expected to form from the ozonolysis of the selected terpenes are summarized in Table 1. When endocyclic C=C double bonds are cleaved, the sCI will retain all the atoms from the terpene and the O_3, thus e.g. α-pinene produces sCIs with the formula $C_{10}H_{16}O_3$. β-pinene only features an exocyclic double bond and the cleavage will form a C_1 or C_9 sCI. According to MCMv3.3.1 (Saunders et al., 2003), the branching ratios for the formation of the C_1 and C_9 CIs are 0.4 and 0.6, respectively, while Ahrens et al. (2014) reports a branching ratio of 0.1 for C_1 and 0.45 each for both C_9 isomers based on infrared spectroscopy experiments. β-caryophyllene has both endo- and exocyclic double bonds and ozone may react with either of these bonds to form either $C_{15}H_{24}O_3$ (endocyclic case) or $CH_2O_2/C_{14}H_{22}O_2$ (exocyclic case). A previous study indicated that ozone predominantly reacts with the endocyclic bond, with the exocyclic reaction being approximately two orders of magnitude slower (Winterhalter et al., 2009).

The ozonolysis of α-pinene forms four isomeric C_{10} sCI, called *syn*-pinonaldehyde oxide, *anti*-pinonaldehyde oxide, *syn*-isopinonaldehyde oxide, and *anti*-isopinonaldehyde oxide (Molecular structures shown in the Supplementary Information). The *syn*- and *anti*-conformers are not interconvertible, but crucially for these experiments, they form the same accretion product, as the non-rotable carbonyl oxide C=O bond is converted into a rotable hydroperoxide C-O bond. Similarly, the β-pinene C_9 sCI has two non-convertible isomers, *syn*-nopinene oxide and *anti*-nopinene oxide, which also form the same accretion products. The latter two form the same accretion product. The β-caryophyllene derived C_{14} and C_{15} sCIs have not been given systematic names as far as we are aware, but the same *syn-anti*-isomerism applies to these as well (Winterhalter et al., 2009; Nguyen et al., 2009).

Table 1. Main sCIs derived from the ozonolysis of the studied terpenes and their corresponding potential accretion products with malonic (MA) and oxalic (OA) acids.

Terpene	sCIs	Potential accretion products with MA	Potential accretion products with OA
α-pinene	$C_{10}H_{16}O_3$	$C_{13}H_{20}O_7$	$C_{12}H_{18}O_7$

β-pinene	CH_2O_2	$C_4H_6O_6$	$C_3H_4O_6$
	$C_9H_{14}O_2$	$C_{12}H_{18}O_6$	$C_{11}H_{16}O_6$
β-caryophyllene	CH_2O_2	$C_4H_6O_6$	$C_3H_4O_6$
	$C_{14}H_{22}O_2$	$C_{17}H_{26}O_6$	$C_{16}H_{24}O_6$
	$C_{15}H_{24}O_3$	$C_{18}H_{28}O_7$	$C_{17}H_{24}O_7$

3.1. Accretion Products Formation in the Flow Reactor

From our previous work on kaurene ozonolysis, we identified C_{21-29} products (Figure 1(a)). The primary sCI from kaurene is expected to be $C_{19}H_{30}O_2$, while we also measured C_{2-9} contaminants in the chamber. If these contaminants were acids and they reacted with the $C_{19}H_{30}O_2$ sCI, several accretion products could be expected to form. To test this, we took the part of the mass spectrum with the contaminants and shifted it by 290 Th (the mass of $C_{19}H_{30}O_2$). As depicted in Figure 1(b), the spectrum aligns almost perfectly with the observed C_{21-29} products. This supports our hypothesis that the observed species were indeed sCI + acid accretion products. In the following sections, we explore this reaction with better controlled experiments.

Figure 2 presents the mass spectra of oxidation products resulting from the ozonolysis of α-pinene, β-pinene, and β-caryophyllene, both with and without the presence of malonic acid. The concentrations of the terpenes and ozone were maintained at similar levels before and after acid injection, ensuring comparable formation of sCIs. Prior to acid injection, we observed many of the typical HOMs associated with the different systems (Ehn et al., 2014; Jokinen et al., 2015; Richters et al., 2016a). For α-pinene, the predominant HOM monomers were $C_{10}H_{14,16}O_{7,9}$, and dimers included $C_{19}H_{28}O_9$, $C_{20}H_{30}O_{12}$, and $C_{20}H_{32}O_{9,11}$. In β-pinene ozonolysis, the major HOM monomers were $C_{10}H_{16}O_{7,8,9}$ and $C_9H_{16}O_6$, with dominant dimers such as $C_{19}H_{28}O_{9,11}$. For β-caryophyllene, the most prevalent HOM monomers were $C_{15}H_{22,24}O_{7,9}$, with dimers including $C_{29}H_{46}O_{12}$ and $C_{30}H_{46}O_{10,12,24}$.

Following the injection of malonic acid, new peaks appeared at the masses corresponding to all the expected accretion products from Table 1 (Figure 2). Notably, no other peaks appeared, strongly indicating that sCI + acid reactions were the driver for the observed changes. For β-caryophyllene, $C_{18}H_{28}O_7$ was clearly the most abundant of the three new products, as expected, but in the β-pinene system, the signal intensity of $C_4H_6O_6$ was more than twice that of $C_{12}H_{18}O_6$. This may indicate that the branching towards the C_1 CI was larger than expected, or that there are differences in the sCI + acid reaction rate coefficients or yields. It is also possible that there is difference in the sensitivity of the NO_3-CIMS towards the different products. For the corresponding oxalic acid experiments, we also detected all expected species at the expected masses for sCIs plus oxalic acid (Figure S2). The largest difference compared to the malonic acid system was that the signal intensities for $C_3H_4O_6$ in β-pinene and $C_{17}H_{26}O_7$ in β-caryophyllene ozonolysis were substantially higher than those of other accretion products. These differences between the two acids were surprising, and for a more detailed look at the dependencies, we study the temporal behaviour of the different species.

Figures S3-S8 display examples of time series for the dominant RO_2, HOM monomers and dimers, acids, and sCIs-derived accretion products in each of the six terpene + acid systems. Comparable observations were made for the systems, and we describe below the β-caryophyllene + malonic acid system (Figure S5 (b)). Without malonic acid, upon introducing ozone into the flow reactor with a stable β-caryophyllene concentration of approximately 30 ppb, the O_3-initiated RO_2 (e.g., $C_{15}H_{23}O_8$) appears immediately, followed by the formation of HOM monomers and dimers. The trends in RO_2, HOM monomers, and dimers correlate well with the ozonolysis rate of β-caryophyllene. Background malonic acid was detected in the flow reactor prior to acid injection, leading to a minor signal of $C_{18}H_{28}O_7$, the accretion product from sCI $C_{15}H_{24}O_3$ and malonic acid. Upon injecting malonic acid at around 13:55, the signal intensity of all the expected accretion products increased around tenfold, while RO_2, HOM monomers, and dimers remained nearly constant, in line with earlier findings that sCI are not intermediates in HOM formation (Richters et al., 2016b). The accretion products also responded as expected to the change of β-caryophyllene and O_3 when the acid level was kept constant. The signal of $C_4H_6O_6$ accumulated throughout the experiment, and only decreased very slowly after the removal of β-caryophyllene and O_3, while all RO_2, HOM, as well as $C_{18}H_{28}O_7$ and $C_{17}H_{26}O_6$ fell below detection limits. A similar pattern was observed for $C_3H_4O_6$ in the oxalic acid system. We interpret this behaviour as these species being semi-volatile, thus accumulating on, and later desorbing from, the wall of the reactor or sampling lines. Similar slow responses were observed also for malonic acid itself. In summary, the temporal trends also are in line with the proposed sCI + acid formation mechanism.

Figure 3 illustrates the relationship between the concentration of accretion products and the ozonolysis rate of terpenes. It is evident that all accretion products, except those from β-caryophyllene ozonolysis sCI CH_2O_2 (Figure S9), track the terpene reaction rate coefficients. The different behaviour of the two accretion products from β-caryophyllene is attributed to their semi-volatile behaviour, as previously mentioned.

In the case of malonic acid (Figure 3(a) & Figure S9 (a)), α-pinene ozonolysis produced the highest concentration of accretion product at a given terpene reaction rate. Although incurring large uncertainties, we can estimate the molar yields of these accretion products, i.e. the fraction of reacted terpene molecules that result in sCI + acid accretion products. For the most abundant products from α-pinene, we estimate yields of ~3 %, while yields of accretion products from β-pinene-derived sCI CH_2O_2 and β-caryophyllene ozonolysis-derived sCI $C_{15}H_{24}O_3$ were comparable at ~1%. Yields from β-pinene-derived sCI $C_9H_{14}O_2$ and β-caryophyllene-derived sCI $C_{14}H_{22}O_2$ were still lower, ~0.5% and ~0.1%, respectively. However, in the oxalic acid case (Figure 3(b) & Figure S9 (b)), most accretion product yields increased dramatically compared to the malonic acid case, except for the β-pinene-derived sCI $C_9H_{14}O_2$ which decreased by a factor of 4. The highest yield was from the β-caryophyllene-derived sCI $C_{15}H_{24}O_3$ at 50%, followed by the α-pinene-derived sCI at 30%. The total yield of accretion products from β-pinene was approximately 5%.

The yields of accretion products discussed above are determined by two key parameters: the stabilization yields of sCIs from the initial ozonolysis reaction and the rates of subsequent sCI + acid reactions. Clearly, the yield of the accretion products cannot exceed the yield of the sCIs from a given system. Earlier studies have reported total sCI yields from α-pinene, β-pinene, and β-caryophyllene ozonolysis to be approximately 15%-34% (Hakala and Donahue, 2023; Sipilä et al., 2014; Zhang and

Zhang, 2005), 22%-70% (Ahrens et al., 2014; Yokouchi and Ambe, 1985; Zhang and Zhang, 2005; Hakala and Donahue, 2023), and ≥60%-74% (Nguyen et al., 2009; Winterhalter et al., 2009; Cox et al., 2020), respectively. This pattern (i.e., β-caryophyllene > β-pinene > α-pinene) diverges from our findings on the accretion product formation, but we also observed significant variations in the yields depending on which dicarboxylic acid we used, with more than a factor 50 difference in the case of β-caryophyllene-derived sCI $C_{15}H_{24}O_3$. In addition, the yields of accretion products from β-pinene-derived sCI CH_2O_2 + acids are higher than products from β-pinene-derived sCI $C_9H_{14}O_2$ + acids, although previous studies have reported higher yields of C_9 sCI than CH_2O_2 sCI in β-pinene ozonolysis (Zhang and Zhang, 2005; Ahrens et al., 2014).

There are several potential explanations for the differences between our results and earlier studies. Firstly, as illustrated in Figure S10, there was not always sufficient acid to fully terminate all the formed sCIs to sCI-acid accretion products, though a significant impact is only expected for the β-caryophyllene + OA case, which already showed a high yield. Another possible explanation is differing detection sensitivities in the NO_3-CIMS. In our computations, the only sCI + acid accretion product (not including the C_{14}-sCI products, for which calculations were not performed) with a lower detection sensitivity was one of the two isomers of the AP-C_{10} + malonic acid, which could explain why the AP-C_{10} + malonic acid signal is one order of magnitude weaker than the AP-C_{10} + oxalic acid signal. However, if both accretion product isomers form in equal amounts the signal should only decrease by a factor of two. Thus, additional explanations are needed.

The above speculations concerned experimental artifacts, but we also looked into possible structural dependencies of sCIs + acid reaction rate coefficients. Previous studies suggest that the simplest sCI reactions with carboxylic acids are barrierless and largely driven by the long-range dipole-dipole interactions (Vereecken et al., 2014; Chhantyal-Pun et al., 2018). We were able to use the dipole moment-based SAR model by Chhantyal-Pun et al. (2018) to estimate relative reaction rate coefficients for the sCI + malonic acid reactions (Section S2), and conclude that these do not explain the observed differences between the AP-C_{10}, BP-C_1 and BP-C_9 signals, as the rate coefficients predict a formation rate ordering of BP-C_9 > BP-C_1 > AP-C_{10}, which is the opposite of what we see, especially when accounting for the terpene-specific total sCI yields. Furthermore, the differences in rate coefficients all fit within a factor of 1.6, which is less than the spread in product formation we see. For the sCI + oxalic acid reactions we were not able to use this model due to the latter molecule's negligible dipole moment, and we instead used collision theory to estimate the rate coefficients (Section S2). While these results similarly imply minimal differences in rate coefficients, we note that the lack of dipole moment means that the relative orientation of the molecules is likely to play a larger role in determining the reaction rate coefficients. We speculate that the reduced signal of the BP-C_9 accretion product in the oxalic acid experiments compared to the malonic acid experiments may be due to such orientation effects, as the bicyclic BP-C_9 is more rigid in its internal motions than AP-C_{10} or CP-C_{14}, and thus may be less likely to spontaneously rotate into the energy slope leading to the reaction. Lastly, differing decomposition of the products, either in the flow tube or inside the mass spectrometer, could result in fragments undetectable with these instruments.

While the ultimate reason for the differing yields estimated in our study and earlier ones remains an open question, we do stress that our main finding is that all the expected accretion products could be detected, and thus we can also look for them in the atmosphere.
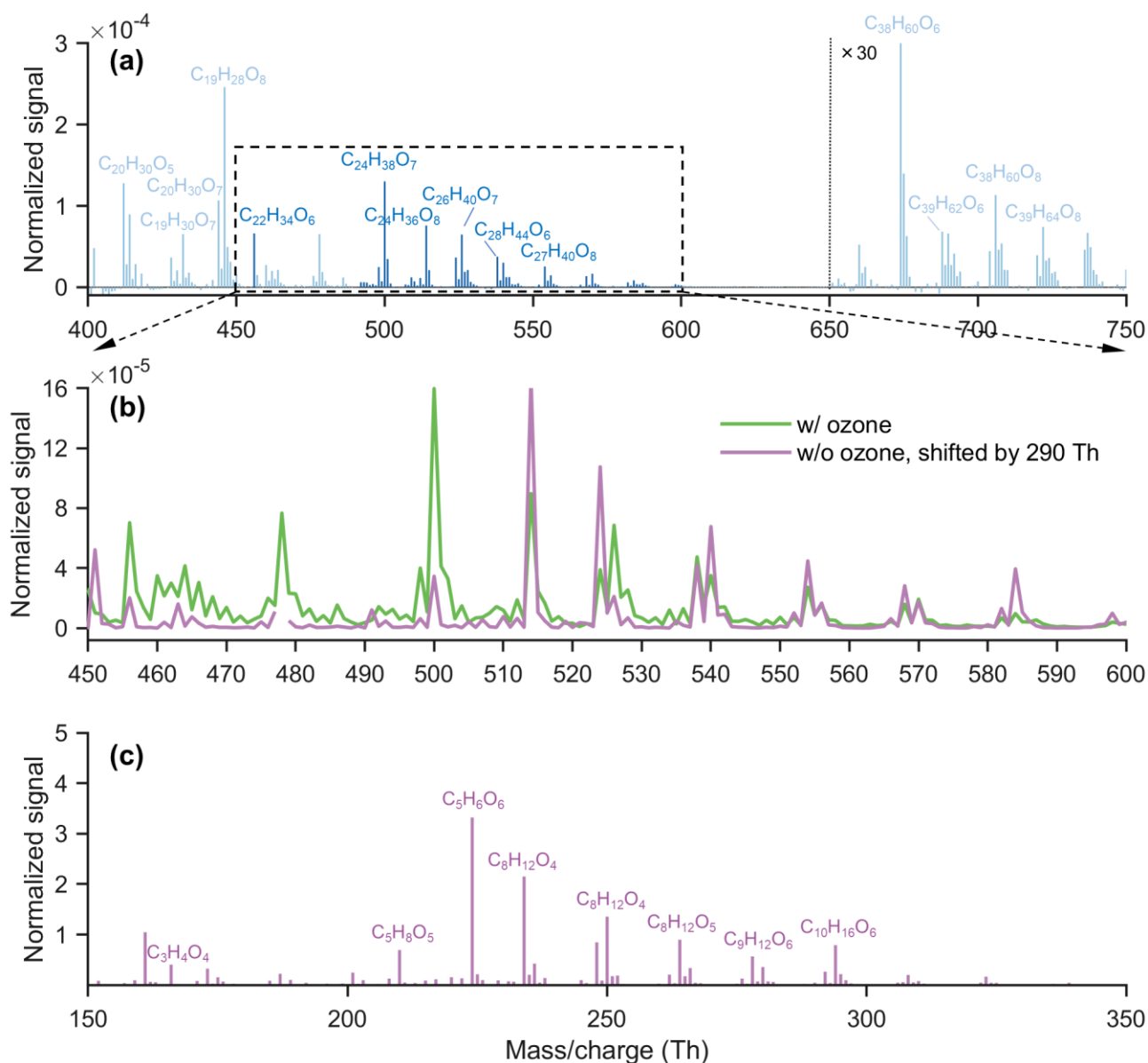
Figure 1. (a) Mass spectrum of HOMs produced by kaurene ozonolysis, with the normalized signal amplified 30-fold in the HOM dimer region (m/z > 650 Th). All peaks were detected as clusters with NO_3^-. (b) Mass spectrum in the m/z range that includes various species with 21-29 C-atoms. The green spectrum represents measurements after ozone injection, while the purple spectrum, indicating chamber background, is the spectrum before ozone injected (panel (c)) shifted by 290 Th (corresponding to the mass of $C_{19}H_{30}O_2$, the main sCI from kaurene ozonolysis) after the signal was reduced by a factor of 200. (c) Mass spectrum of chamber background before ozone injection.

245
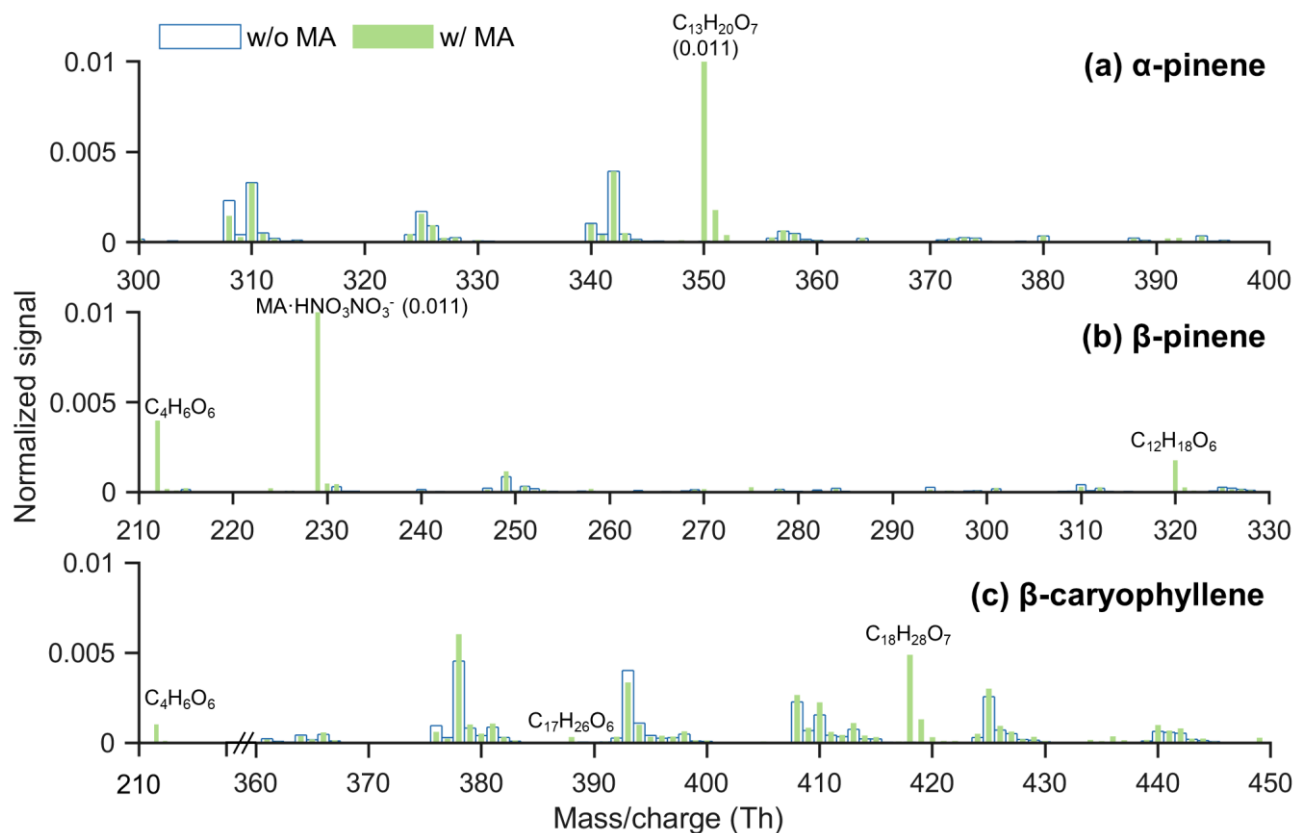
Figure 2. Mass spectrum of products formed from the ozonolysis of (a) α-pinene, (b) β-pinene, and (c) β-caryophyllene, both with and without the presence of malonic acid. New peaks are labeled with their identified compositions and numbers in parentheses denote signal strengths when peaks go off-scale.
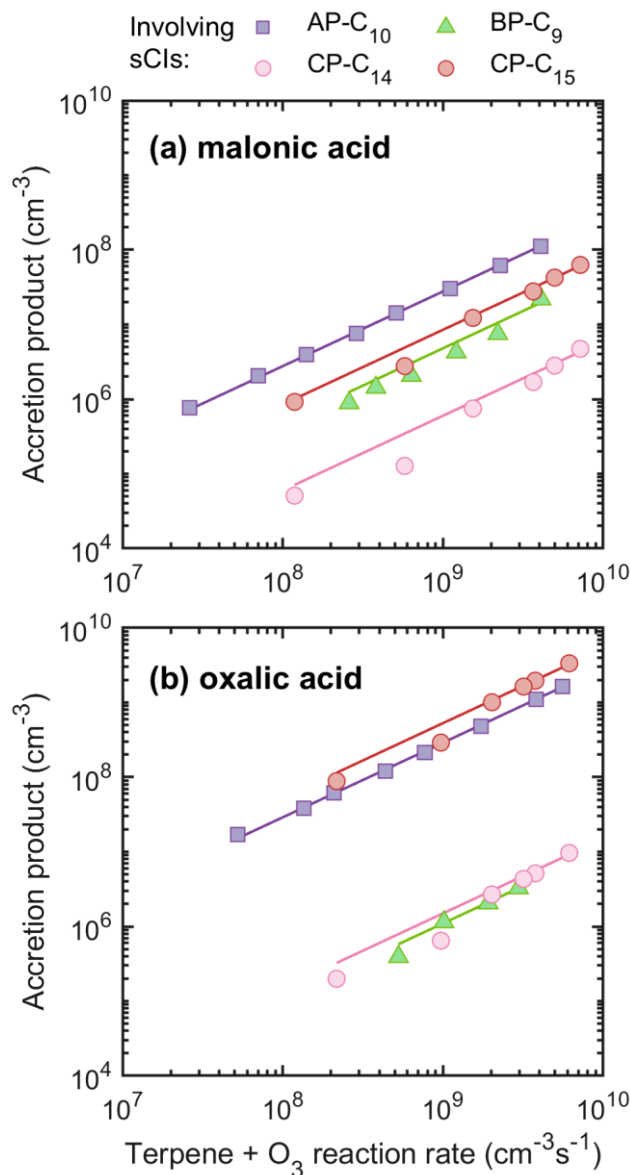
Figure 3. Concentrations of accretion products from sCIs with (a) malonic acid and (b) oxalic acid plotted against the ozonolysis rate of terpenes. The lines represent linear fits. Legend labels indicate different accretion products formed from various sCIs in reaction with the acids. For instance, AP-C_{10} in panel (a) corresponds to the accretion product $C_{13}H_{20}O_7$, formed from the sCI $C_{10}H_{16}O_3$ with malonic acid; similarly, AP-C_{10} in panel (b) corresponds to the accretion product $C_{12}H_{18}O_7$, formed from the same sCI reacting with oxalic acid.

3.2. Potential Accretion Product Observations in the Ambient Air

A NO$_3$-CIMS is permanently deployed at the Station for Measuring Ecosystem-Atmosphere Relations (SMEAR II) in Hyytiälä, Southern Finland, to monitor low-volatility species. We analyzed data during late spring to summer (May 01 to August 31, 2023) to investigate potential accretion products from monoterpene sCIs and organic acids, as monoterpene oxidation products have been shown to dominate the HOM spectrum at this site (Yan et al., 2016; Ehn et al., 2012; Lee et al., 2018). The time resolution of data in Hyytiälä is 30 min.

Measurements in Hyytiälä revealed a series of species whose chemical formulas corresponded to the mass of the α-pinene ozonolysis-derived sCI $C_{10}H_{16}O_3$ combined with malonic, oxalic, or formic acid. As demonstrated in Figure S11, these potential accretion products correlated well with the respective acids during the whole observation period. The most abundant species was $C_{11}H_{18}O_5$, which corresponds to the composition of the adduct of sCI $C_{10}H_{16}O_3$ and formic acid. Given that formic acid was one of the most prevalent organic acids measured in the ambient environment (Stavrakou et al., 2012; Millet et al., 2015), its adduction with the sCI is possible, despite NO$_3$-CIMS's inability to detect formic acid directly. Malonic acid signals were significantly higher than those of oxalic acid, likely due to a higher detection efficiency of malonic acid in the NO$_3$-CIMS (Ehn et al., 2012) but the levels of $C_{13}H_{20}O_7$ and $C_{12}H_{18}O_7$ were almost comparable. Despite these observations, a good correlation (Figure S12) was also observed between these acids and various other C_{12} and C_{13} species. While it is possible that the discussed species are from sCI + acid reactions, it must be kept in mind that similar diurnal cycles can be caused by many different types of processes. Consequently, we cannot definitively conclude that these species are accretion products of sCIs with organic acids.

4. Conclusions

This study examined the reactions between sCIs and carboxylic acids to assess their potential to form low-volatility accretion products. Utilizing a flow reactor, we investigated the ozonolysis of three terpenes—α-pinene, β-pinene, and β-caryophyllene—combined with malonic and oxalic acids. We detected the expected accretion products from sCIs + acid in all systems. Our findings indicate that accretion products from sCIs + acids formed readily, with specific variances across different terpenes and acids. For instance, α-pinene ozonolysis yielded the most significant accretion product concentration with malonic acid. Conversely, β-caryophyllene ozonolysis with oxalic acid resulted in the highest yield among the tested combinations. These experimental results validate the hypothesis that sCIs originating from the ozonolysis of terpenes can significantly interact with organic acids forming accretion products but leave open questions regarding the yields between given sCI-acid pairs.

To our knowledge, this study is the first to show direct observations of gas-phase accretion products from terpene sCIs + acid reactions. The high efficiency of these reactions implies that sCIs could influence the dynamics and composition of organic aerosol formation in the troposphere, but future studies should look into the rate coefficients of suppression of the accretion products at different levels of humidity.

290   **Data availability.** Data is available upon request by contacting the corresponding authors.

Author Contributions. The laboratory experiments and data analysis were conducted by YL. LF conducted the quantum calculation. JZ performed the analysis of data from ambient air. YL prepared the original draft with larger contributions from LF. All authors contributed to the discussion and comment on the manuscript.

Competing interests. The authors declare that they have no conflict of interest.

295   **Acknowledgments.** This research received support from the Academy of Finland (grant nos. 317380 and 320094), and the China Scholarship Council (grant no. 201906220191) for YL.

References

Ahrens, J., Carlsson, P. T., Hertl, N., Olzmann, M., Pfeifle, M., Wolf, J. L., and Zeuch, T.: Infrared detection of Criegee intermediates formed during the ozonolysis of β-pinene and their reactivity towards sulfur dioxide, Angewandte Chemie International Edition, 53, 715-719, https://doi.org/10.1002/anie.201307327, 2014.

Berndt, T., Herrmann, H., and Kurtén, T.: Direct Probing of Criegee Intermediates from Gas-Phase Ozonolysis Using Chemical Ionization Mass Spectrometry, Journal of the American Chemical Society, 139, 13387-13392, 10.1021/jacs.7b05849, 2017.

Berndt, T., Mentler, B., Scholz, W., Fischer, L., Herrmann, H., Kulmala, M., and Hansel, A.: Accretion Product Formation from Ozonolysis and OH Radical Reaction of α-Pinene: Mechanistic Insight and the Influence of Isoprene and Ethylene, Environmental Science & Technology, 52, 11069-11077, 10.1021/acs.est.8b02210, 2018.

Chebbi, A. and Carlier, P.: Carboxylic acids in the troposphere, occurrence, sources, and sinks: A review, Atmospheric Environment, 30, 4233-4249, https://doi.org/10.1016/1352-2310(96)00102-1, 1996.

Chhantyal-Pun, R., Davey, A., Shallcross, D. E., Percival, C. J., and Orr-Ewing, A. J.: A kinetic study of the CH 2 OO Criegee intermediate self-reaction, reaction with SO 2 and unimolecular reaction using cavity ring-down spectroscopy, Physical Chemistry Chemical Physics, 17, 3617-3626, 10.1039/C4CP04198D 2015.

Chhantyal-Pun, R., Khan, M. A. H., Taatjes, C. A., Percival, C. J., Orr-Ewing, A. J., and Shallcross, D. E.: Criegee intermediates: production, detection and reactivity, International Reviews in Physical Chemistry, 39, 385-424, **https://doi.org/10.1080/0144235X.2020.1792104**, 2020.

Chhantyal-Pun, R., Rotavera, B., McGillen, M. R., Khan, M. A. H., Eskola, A. J., Caravan, R. L., Blacker, L., Tew, D. P., Osborn, D. L., Percival, C. J., Taatjes, C. A., Shallcross, D. E., and Orr-Ewing, A. J.: Criegee Intermediate Reactions with Carboxylic Acids: A Potential Source of Secondary Organic Aerosol in the Atmosphere, ACS Earth and Space Chemistry, 2, 833-842, 10.1021/acsearthspacechem.8b00069, 2018.

Chhantyal-Pun, R., McGillen, M. R., Beames, J. M., Khan, M. A. H., Percival, C. J., Shallcross, D. E., and Orr-Ewing, A.: Temperature-Dependence of the Rates of Reaction of Trifluoroacetic Acid with Criegee Intermediates, Angewandte Chemie, 129, 9172-9175, https://doi.org/10.1002/ange.201703700, 2017.

Cox, R. A., Ammann, M., Crowley, J. N., Herrmann, H., Jenkin, M. E., McNeill, V. F., Mellouki, A., Troe, J., and Wallington, T. J.: Evaluated kinetic and photochemical data for atmospheric chemistry: Volume VII – Criegee intermediates, Atmos. Chem. Phys., 20, 13497-13519, 10.5194/acp-20-13497-2020, 2020.

Drozd, G. T. and Donahue, N. M.: Pressure Dependence of Stabilized Criegee Intermediate Formation from a Sequence of Alkenes, The Journal of Physical Chemistry A, 115, 4381-4387, 10.1021/jp2001089, 2011.

Ehn, M., Thornton, J. A., Kleist, E., Sipilä, M., Junninen, H., Pullinen, I., Springer, M., Rubach, F., Tillmann, R., and Lee, B.: A large source of low-volatility secondary organic aerosol, Nature, 506, 476-479, https://doi.org/10.1038/nature13032, 2014.

Ehn, M., Kleist, E., Junninen, H., Petäjä, T., Lönn, G., Schobesberger, S., Dal Maso, M., Trimborn, A., Kulmala, M., Worsnop, D. R., Wahner, A., Wildt, J., and Mentel, T. F.: Gas phase formation of extremely oxidized pinene reaction products in chamber and ambient air, Atmospheric Chemistry and Physics, 12, 5113-5127, https://doi.org/10.5194/acp-12-5113-2012, 2012.

Elsamra, R. M., Jalan, A., Buras, Z. J., Middaugh, J. E., and Green, W. H.: Temperature-and pressure-dependent kinetics of CH2OO+ CH3COCH3 and CH2OO+ CH3CHO: direct measurements and theoretical analysis, International Journal of Chemical Kinetics, 48, 474-488, https://doi.org/10.1002/kin.21007, 2016.

Faiola, C. L., Buchholz, A., Kari, E., Yli-Pirilä, P., Holopainen, J. K., Kivimäenpää, M., Miettinen, P., Worsnop, D. R., Lehtinen, K. E. J., Guenther, A. B., and Virtanen, A.: Terpene Composition Complexity Controls Secondary Organic Aerosol Yields from Scots Pine Volatile Emissions, Scientific Reports, 8, 3053, 10.1038/s41598-018-21045-1, 2018.

Gong, Y. and Chen, Z.: Quantification of the role of stabilized Criegee intermediates in the formation of aerosols in limonene ozonolysis, Atmospheric Chemistry and Physics, 21, 813-829, 10.5194/acp-21-813-2021, 2021.

Gong, Y., Jiang, F., Li, Y., Leisner, T., and Saathoff, H.: Impact of temperature on the role of Criegee intermediates and peroxy radicals in dimer formation from β-pinene ozonolysis, Atmospheric Chemistry and Physics, 24, 167-184, 10.5194/acp-24-167-2024, 2024.

Hakala, J. and Donahue, N. M.: Carbonyl Oxide Stabilization from Trans Alkene and Terpene Ozonolysis, The Journal of Physical Chemistry A, 127, 8530-8543, 10.1021/acs.jpca.3c03650, 2023.

Hyttinen, N., Kupiainen-Määttä, O., Rissanen, M. P., Muuronen, M., Ehn, M., and Kurtén, T.: Modeling the Charging of Highly Oxidized Cyclohexene Ozonolysis Products Using Nitrate-Based Chemical Ionization, The Journal of Physical Chemistry A, 119, 6339-6345, https://doi.org/10.1021/acs.jpca.5b01818, 2015.

Jokinen, T., Berndt, T., Makkonen, R., Kerminen, V. M., Junninen, H., Paasonen, P., Stratmann, F., Herrmann, H., Guenther, A. B., Worsnop, D. R., Kulmala, M., Ehn, M., and Sipila, M.: Production of extremely low volatile organic compounds from biogenic emissions: Measured yields and atmospheric implications, The Proceedings of the National Academy of Sciences, 112, 7123-7128, https://doi.org/10.1073/pnas.1423977112, 2015.

Junninen, H.: Data cycle in atmospheric physics: From detected millivolts to understanding the atmosphere, University of Helsinki, 2014.

Junninen, H., Ehn, M., Petäjä, T., Luosujärvi, L., Kotiaho, T., Kostiainen, R., Rohner, U., Gonin, M., Fuhrer, K., Kulmala, M., and Worsnop, D. R.: A high-resolution mass spectrometer to measure atmospheric ion composition, Atmospheric Measurement Techniques, 3, 1039-1053, https://doi.org/10.5194/amt-3-1039-2010, 2010.

355   Kawamura, K., Ng, L. L., and Kaplan, I. R.: Determination of organic acids (C1-C10) in the atmosphere, motor exhausts, and engine oils, Environmental science technology, 19, 1082-1086, 0013-936X/85/0919-1082$01.50/0, 1985.

Khan, M., Percival, C., Caravan, R., Taatjes, C., and Shallcross, D.: Criegee intermediates and their impacts on the troposphere, Environmental Science: Processes Impacts, 20, 437-453, 10.1039/C7EM00585G, 2018.

Khan, M. A. H., Cooke, M. C., Utembe, S. R., Xiao, P., Morris, W. C., Derwent, R. G., Archibald, A. T., Jenkin, M. E., Percival, C. J., and

360   Shallcross, D. E.: The global budgets of organic hydroperoxides for present and pre-industrial scenarios, Atmospheric Environment, 110, 65-74, https://doi.org/10.1016/j.atmosenv.2015.03.045, 2015.

Krechmer, J., Lopez-Hilfiker, F., Koss, A., Hutterli, M., Stoermer, C., Deming, B., Kimmel, J., Warneke, C., Holzinger, R., Jayne, J., Worsnop, D., Fuhrer, K., Gonin, M., and de Gouw, J.: Evaluation of a New Reagent-Ion Source and Focusing Ion-Molecule Reactor for Use in Proton-Transfer-Reaction Mass Spectrometry, Analytical Chemistry, 90, 12011-12018, https://doi.org/10.1021/acs.analchem.8b02641,

365   2018.

Lee, A., Goldstein, A. H., Kroll, J. H., Ng, N. L., Varutbangkul, V., Flagan, R. C., and Seinfeld, J. H.: Gas-phase products and secondary aerosol yields from the photooxidation of 16 different terpenes, Journal of Geophysical Research: Atmospheres, 111, https://doi.org/10.1029/2006JD007050, 2006.

Lee, B. H., Lopez-Hilfiker, F. D., D'Ambro, E. L., Zhou, P., Boy, M., Petäjä, T., Hao, L., Virtanen, A., and Thornton, J. A.: Semi-volatile

370   and highly oxygenated gaseous and particulate organic compounds observed above a boreal forest canopy, Atmospheric Chemistry and Physics, 18, 11547-11562, 10.5194/acp-18-11547-2018, 2018.

Lester, M. I. and Klippenstein, S. J.: Unimolecular Decay of Criegee Intermediates to OH Radical Products: Prompt and Thermal Decay Processes, Accounts of Chemical Research, 51, 978-985, 10.1021/acs.accounts.8b00077, 2018.

Lin, J. J.-M. and Chao, W.: Structure-dependent reactivity of Criegee intermediates studied with spectroscopic methods, Chemical Society

375   Reviews, 46, 7483-7497, DOI: 10.1039/c7cs00336f, 2017.

Long, B., Bao, J. L., and Truhlar, D. G.: Atmospheric Chemistry of Criegee Intermediates: Unimolecular Reactions and Reactions with Water, Journal of the American Chemical Society, 138, 14409-14422, 10.1021/jacs.6b08655, 2016.

Luo, Y., Garmash, O., Li, H., Graeffe, F., Praplan, A. P., Liikanen, A., Zhang, Y., Meder, M., Peräkylä, O., Peñuelas, J., Yáñez-Serrano, A. M., and Ehn, M.: Oxidation product characterization from ozonolysis of the diterpene ent-kaurene, Atmospheric Chemistry and Physics, 22,

380   5619-5637, 10.5194/acp-22-5619-2022, 2022.

Millet, D. B., Baasandorj, M., Farmer, D. K., Thornton, J. A., Baumann, K., Brophy, P., Chaliyakunnel, S., de Gouw, J. A., Graus, M., Hu, L., Koss, A., Lee, B. H., Lopez-Hilfiker, F. D., Neuman, J. A., Paulot, F., Peischl, J., Pollack, I. B., Ryerson, T. B., Warneke, C., Williams, B. J., and Xu, J.: A large and ubiquitous source of atmospheric formic acid, Atmospheric Chemistry and Physics, 15, 6283-6304, 10.5194/acp-15-6283-2015, 2015.

385   Neese, F.: Software update: The ORCA program system—Version 5.0, Wiley Interdisciplinary Reviews: Computational Molecular Science, 12, e1606, https://doi.org/10.1002/wcms.1606, 2022.

Neese, F.: The SHARK integral generation and digestion system, Journal of Computational Chemistry, 44, 381-396, https://doi.org/10.1002/jcc.26942, 2023.

Nguyen, T. L., Winterhalter, R., Moortgat, G., Kanawati, B., Peeters, J., and Vereecken, L.: The gas-phase ozonolysis of β-caryophyllene

390   (C 15 H 24). Part II: A theoretical study, Physical Chemistry Chemical Physics, 11, 4173-4183, 10.1039/b817913a, 2009.

Osborn, D. L. and Taatjes, C. A.: The physical chemistry of Criegee intermediates in the gas phase, International Reviews in Physical Chemistry, 34, 309-360, 10.1080/0144235X.2015.1055676, 2015.

Pracht, P., Grimme, S., Bannwarth, C., Bohle, F., Ehlert, S., Feldmann, G., Gorges, J., Müller, M., Neudecker, T., and Plett, C.: CREST— A program for the exploration of low-energy molecular chemical space, The Journal of Chemical Physics, 160,

395   https://doi.org/10.1063/5.0197592, 2024.

Richters, S., Herrmann, H., and Berndt, T.: Highly Oxidized RO2 Radicals and Consecutive Products from the Ozonolysis of Three Sesquiterpenes, Environment Science & Technology, 50, 2354-2362, https://doi.org/10.1021/acs.est.5b05321, 2016a.

Richters, S., Herrmann, H., and Berndt, T.: Different pathways of the formation of highly oxidized multifunctional organic compounds (HOMs) from the gas-phase ozonolysis of β-caryophyllene, Atmospheric Chemistry and Physics, 16, 9831-9845, 10.5194/acp-16-9831-

400   2016, 2016b.

Riva, M., Rantala, P., Krechmer, J. E., Peräkylä, O., Zhang, Y., Heikkinen, L., Garmash, O., Yan, C., Kulmala, M., Worsnop, D., and Ehn, M.: Evaluating the performance of five different chemical ionization techniques for detecting gaseous oxygenated organic species, Atmospheric Measurement Techniques, 12, 2403-2421, https://doi.org/10.5194/amt-12-2403-2019, 2019.

Saunders, S. M., Jenkin, M. E., Derwent, R. G., and Pilling, M. J.: Protocol for the development of the Master Chemical Mechanism, MCM

405   v3 (Part A): tropospheric degradation of non-aromatic volatile organic compounds, Atmospheric Chemistry and Physics, 3, 161-180, 10.5194/acp-3-161-2003, 2003.

Sheps, L., Scully, A. M., and Au, K.: UV absorption probing of the conformer-dependent reactivity of a Criegee intermediate CH 3 CHOO, Physical Chemistry Chemical Physics, 16, 26701-26706, 10.1039/c4cp04408h, 2014.

Sipilä, M., Jokinen, T., Berndt, T., Richters, S., Makkonen, R., Donahue, N. M., Mauldin Iii, R. L., Kurtén, T., Paasonen, P., Sarnela, N., Ehn, M., Junninen, H., Rissanen, M. P., Thornton, J., Stratmann, F., Herrmann, H., Worsnop, D. R., Kulmala, M., Kerminen, V. M., and Petäjä, T.: Reactivity of stabilized Criegee intermediates (sCIs) from isoprene and monoterpene ozonolysis toward SO$_2$ and organic acids, Atmospheric Chemistry and Physics, 14, 12143-12153, 10.5194/acp-14-12143-2014, 2014.

Stavrakou, T., Müller, J. F., Peeters, J., Razavi, A., Clarisse, L., Clerbaux, C., Coheur, P. F., Hurtmans, D., De Mazière, M., Vigouroux, C., Deutscher, N. M., Griffith, D. W. T., Jones, N., and Paton-Walsh, C.: Satellite evidence for a large source of formic acid from boreal and tropical forests, Nature Geoscience, 5, 26-30, 10.1038/ngeo1354, 2012.

Taatjes, C. A., Welz, O., Eskola, A. J., Savee, J. D., Scheer, A. M., Shallcross, D. E., Rotavera, B., Lee, E. P. F., Dyke, J. M., Mok, D. K. W., Osborn, D. L., and Percival, C. J.: Direct Measurements of Conformer-Dependent Reactivity of the Criegee Intermediate CH3CHOO, Science, 340, 177-180, 10.1126/science.1234689, 2013.

Vansco, M. F., Caravan, R. L., Pandit, S., Zuraski, K., Winiberg, F. A., Au, K., Bhagde, T., Trongsiriwat, N., Walsh, P. J., and Osborn, D. L.: Formic acid catalyzed isomerization and adduct formation of an isoprene-derived Criegee intermediate: experiment and theory, Physical Chemistry Chemical Physics, 22, 26796-26805, 10.1039/D0CP05018K, 2020.

Vereecken, L.: The reaction of Criegee intermediates with acids and enols, Physical Chemistry Chemical Physics, 19, 28630-28640, 10.1039/C7CP05132H, 2017.

Vereecken, L. and Francisco, J. S.: Theoretical studies of atmospheric reaction mechanisms in the troposphere, Chemical Society Reviews, 41, 6259-6293, 10.1039/C2CS35070J, 2012.

Vereecken, L., Harder, H., and Novelli, A.: The reactions of Criegee intermediates with alkenes, ozone, and carbonyl oxides, Physical Chemistry Chemical Physics, 16, 4039-4049, 10.1039/C3CP54514H, 2014.

Wang, M., Yao, L., Zheng, J., Wang, X., Chen, J., Yang, X., Worsnop, D. R., Donahue, N. M., and Wang, L.: Reactions of Atmospheric Particulate Stabilized Criegee Intermediates Lead to High-Molecular-Weight Aerosol Components, Environmental Science & Technology, 50, 5702-5710, 10.1021/acs.est.6b02114, 2016.

Welz, O., Savee, J. D., Osborn, D. L., Vasu, S. S., Percival, C. J., Shallcross, D. E., and Taatjes, C. A.: Direct Kinetic Measurements of Criegee Intermediate (CH2OO) Formed by Reaction of CH2O2, Science, 335, 204-207, doi:10.1126/science.1213229, 2012.

Welz, O., Eskola, A. J., Sheps, L., Rotavera, B., Savee, J. D., Scheer, A. M., Osborn, D. L., Lowe, D., Murray Booth, A., and Xiao, P.: Rate coefficients of C1 and C2 Criegee intermediate reactions with formic and acetic acid near the collision limit: direct kinetics measurements and atmospheric implications, Angewandte Chemie International Edition, 53, 4547-4550, https://doi.org/10.1002/anie.201400964, 2014.

Winterhalter, R., Herrmann, F., Kanawati, B., Nguyen, T. L., Peeters, J., Vereecken, L., and Moortgat, G. K.: The gas-phase ozonolysis of β-caryophyllene (C 15 H 24). Part I: an experimental study, Physical Chemistry Chemical Physics, 11, 4152-4172, 10.1039/b817824k, 2009.

Yan, C., Nie, W., Äijälä, M., Rissanen, M. P., Canagaratna, M. R., Massoli, P., Junninen, H., Jokinen, T., Sarnela, N., Häme, S. A. K., Schobesberger, S., Canonaco, F., Yao, L., Prévôt, A. S. H., Petäjä, T., Kulmala, M., Sipilä, M., Worsnop, D. R., and Ehn, M.: Source characterization of highly oxidized multifunctional compounds in a boreal forest environment using positive matrix factorization, Atmospheric Chemistry and Physics, 16, 12715-12731, 10.5194/acp-16-12715-2016, 2016.

Yang, W., Cao, J., Wu, Y., Kong, F., and Li, L.: Review on plant terpenoid emissions worldwide and in China, Science of The Total Environment, 787, 147454, https://doi.org/10.1016/j.scitotenv.2021.147454, 2021.

Yao, L., Ma, Y., Wang, L., Zheng, J., Khalizov, A., Chen, M., Zhou, Y., Qi, L., and Cui, F.: Role of stabilized Criegee Intermediate in secondary organic aerosol formation from the ozonolysis of α-cedrene, Atmospheric Environment, 94, 448-457, https://doi.org/10.1016/j.atmosenv.2014.05.063, 2014.

Yokouchi, Y. and Ambe, Y.: Aerosols formed from the chemical reaction of monoterpenes and ozone, Atmospheric Environment, 19, 1271-1276, https://doi.org/10.1016/0004-6981(85)90257-4, 1985.

Zhang, D. and Zhang, R.: Ozonolysis of α-pinene and β-pinene: kinetics and mechanism, The Journal of chemical physics, 122, https://doi.org/10.1063/1.1862616, 2005.